Amino Acids (2014) 46:1649–1657
DOI 10.1007/s00726-014-1724-0

ORIGINAL ARTICLE

Immobilized papain on gold nanorods as heterogeneous biocatalysts

Ahmad Homaei · Hossein Barkheh · Reyhaneh Sariri · Roberto Stevanato

Received: 13 September 2013 / Accepted: 6 March 2014 / Published online: 23 March 2014

Abstract Papain, a thiol protease present in the latex of Carica papaya, is an enzyme which exhibits broad proteolytic activity, and, for this reason, it is utilized in a variety of industrial applications. Immobilization of papain on gold nanoparticles highly preserves its activity and enhances the stability, allowing the reuse of the linked enzyme many times without any significant loss of its catalytic performance. In particular, k_{cat} and K_M values remain substantially unchanged, while immobilized form shows a higher activity on a wider pH range retains 80 % residual activity also at 90 °C and shows higher functionality than the free form when incubated for long time (1 h) at 90 °C and at extreme pH values (3 and 12). A higher activity of immobilized papain with respect to the free form in the presence of various bivalent metal ions, known as strong inhibitors of papain, was also found. The reasons of this enhanced stability of gold nanorods immobilized papain are discussed.

A. Homaei (✉)
Department of Biology, Faculty of Sciences, University of Hormozgan, Bandar Abbas, Iran
e-mail: a.homaei@hormozgan.ac.ir

H. Barkheh
Cellular and Molecular Research Center, Yasuj University of Medical Sciences, Yasuj, Iran

R. Sariri
Lahijan Branch, Department of Microbiology, Islamic Azad University, Lahijan, Iran

R. Stevanato (✉)
Department of Molecular Sciences and Nanosystems, University Ca' Foscari of Venice, Venice, Italy
e-mail: rstev@unive.it; roberto.stevanato@unive.it

Keywords Nanorods · Papain · Enzyme immobilization · Electrostatic and hydrophobic interactions

Introduction

Nanoparticles of gold offer a number of fruitful applications, making them appropriate for a variety of biological studies; they show strong optical absorption and their surface chemistry allows straightforward attachment of organic molecules tailored for specific purposes (Talbert and Goddard 2012). In addition, the surface of the nanorods can be functionalized by a very wide variety of molecules. This has led to interest in their use as selective biomarkers in biodiagnostics or for selective targeting in photothermal therapeutics. Gold nanorods are known to exhibit promising applications in therapeutics and diagnostics (Pissuwan et al. 2008). Due to their unique nature, these rod-shaped nanostructures have rapidly found broad place in biological and biomedical applications. The sensitivity of the surface plasmon resonance (SPR) bands to the local environment is quite important in terms of biological sensing (Huang et al. 2009). The rod morphology of these nanostructures induces unique optical properties, including two strong surface plasmon absorption bands (Huang et al. 2009; Sau et al. 2004).

Some of the important application of gold nanorods include selective therapeutic agents (Pissuwan et al. 2008; Li et al. 2009; Pissuwan et al. 2011), non-viral gene carriers (Takahashi et al. 2005; Chen et al. 2006), photothermal therapy (Dickerson et al. 2008), toxicity enhancers in cancer chemotherapeutics (Hauck et al. 2008), diagnostic agents (He et al. 2008) and nanobiosensors (Yu and Irudayaraj 2007). Moreover, gold nanorods possess strong binding affinity to thiol groups, which helps in efficient

conjugation with biomolecules (Huang et al. 2009). Functionalization of these rod-shaped nanostructures with antibodies or other biomolecules also allows specific attachment to any target cell of interest, manifesting a low level of toxicity in the biological systems (Huang et al. 2009). On the other hand, adsorption of proteins on the nanoparticle surface might affect the characteristic conformation and function of the biomolecules (Larsericsdotter et al. 2001; Roach et al. 2005) depending on the nature of the adsorbed biomolecules as well as the physicochemical properties of the nanoparticle surface (Larsericsdotter et al. 2001; Roach et al. 2005; Billsten et al. 1999). Up to the present time, little is known about the conformation, enzymatic activity, binding site, kinetic and thermodynamic stability of biomolecules that interact with nanoparticles (Chakraborti et al. 2010). The catalytic efficacy of papain by immobilizing onto magnetic gold nanocomposite, with concomitant enhancement in enzyme immobilization efficiency, activity, and storage stability opens up new avenues in biotechnological applications. The magnetic gold nanocomposites have been fabricated for the successful immobilization of an industrially important enzyme "papain" (Sahoo et al. 2013).

A nanocomposite consisting of magnetite nanoparticles (Fe_3O_4NPs) and Au nanoparticles (AuNPs) embedded on cellulose nanocrystals (CNCs) was used as a magnetic support for the covalent conjugation of papain and facilitated recovery of this immobilized enzyme. The nanocomposite was successfully used for the immobilization and separation of papain from the reaction mixture (Mahmoud et al. 2013).

Trypsin was either attached directly via hydrophobic and ionic interactions onto the citrate stabilized GNPs or immobilized via EDC/NHS bioconjugation onto the carboxylic functionalized GNPs, respectively (Hinterwirth et al. 2012). The separation, reusability and high catalytic activity of bioconjugate remain challenging task in proteins bound gold nanoparticles. A facile synthetic route for the fabrication of gold nanoparticle assembled polyurethane microsphere template and immobilization of trypsin on gold/polyurethane surface to form trypsin–nanogold–polyurethane bioconjugate was developed (Kotal 2011). Nanomaterials may interact with biomolecules in various ways and change their bioactivities. It is reported on how gold nanoparticles (AuNPs) affect a most important protease, trypsin. The further protease assay of trypsin, before and after mixing with the AuNPs solution, pointed out an improved performance in terms of enzyme activity and stability (Lv et al. 2009). Fluorescent-labeled antibodies and DNA are hydrolyzed on the surface of the nanoparticles by the addition of trypsin and DNase I, respectively, resulting in the release of the quantifiable fluorescent label into the bulk solution (McKenzie 2009).

Papain, a thiol protease present in the latex of Carica papaya, is an enzyme of high research interest due to its ability to be utilized in a variety of industrial applications. In the food industry, papain is used to tenderize meat, to produce protein hydrolysate and to clarify juice. It also has broad applications for cheese production in dairy industry and for the extraction of flavor and color compounds from plants. The immobilized form of papain shows advantageous characteristics with respect to its soluble form (Homaei et al. 2010). A problem in enzyme immobilization is the loss of enzyme activity, which is attributed to many factors involving enzyme, matrix, reagents and process conditions (Delanoy et al. 2005; Rao et al. 2006). Several strategies have been employed to improve the catalytic activity of immobilized enzymes, including contemporary immobilization of the enzyme and its activator (Homaei et al. 2010), use of oriented mode of binding (Hipwell et al. 1974; Wilchek and Miron 2003), chemical post-immobilization techniques (Blanco and Guisan 1992; Rocha et al. 1998) and manipulating the structure of carrier materials (Kim et al. 2006).

To the best of our knowledge, studies of cysteine protease immobilized on gold nanorods have rarely been reported. In this paper, gold nanorods were prepared by sequential seed mediated growth method. Papain was immobilized on gold nanorods and conditions for the immobilization and characterizations of the immobilization enzyme were specified. The efficacy of immobilization was determined by measuring papain activity and stability and comparing the data with those obtained utilizing its soluble form. It is expected that the results presented in this paper would provide a sound basis to further investigations.

Materials and methods

Chemicals

All chemicals were reagent grade and purchased from Merck (Darmstadt, Germany).

Preparation and characterization of gold nanorods

Short gold nanorods were synthesized via sequential seed mediated growth method. The protocol has been formerly described in previous papers (Talbert and Goddard 2012; Nikoobakht and El-sayed 2003; Gole and Murphy 2004; Choma et al. 2012). The procedure starts with preparation of small spherical gold nanoparticles of size below 5 nm (to be used as seeds). In a test tube, 250 μL of an aqueous 10 mM solution of $HAuCl_4 \cdot 3H_2O$ was added to 7.5 mL of a 95 mM cetyltrimethylammonium bromide (CTAB) solution. Immediately, 600 μL of 10 mM ice-cold $NaBH_4$

aqueous solution was added and the reactants were mixed by rapid inversion for 2 min. Meanwhile, evolved gas was allowed to escape at the time of mixing. The solution developed a pale brown-yellow color. The test tube was then incubated at room temperature for at least 2 h to permit seed particles to grow.

In a typical experiment of growth stage, 9.5 mL of 95 mM CTAB, 400 μL of 10 mM $HAuCl_4 \cdot 3H_2O$ and 60 μL of 10 mM $AgNO_3$ solutions were added, respectively, and mixed very gently. At this stage an intense color was produced. The procedure was continued by adding 64 μL of 100 mM ascorbic acid, which further reduced gold, and the appearance of solution was changed to colorless. Finally, 40 μL of seed particles were added. The reaction mixture in the test tube was shaken gently for 10 s and kept undisturbed for 3 h. Intense purple-brown color started to appear within few minutes. The suspension was repeatedly centrifuged (12,000 rpm, 6 min) and gold nanorods sample washed alternatively with deionized water and phosphate buffer pH 7.5. Concentration of the purified gold nanorods was 30 nm.

All subsequent measurements, characterizations and interactions were conducted using the same GNR samples.

Transmission electron microscopy (TEM) investigation was performed with a TE 2000 Zeiss electron microscope. The sample, previously purified by centrifugation, was re-dispersed in deionized water and a dilute sample was deposited on a carbon coated copper grid and left some time to permit solvent evaporation. Gold nanorods were also characterized by UV–Vis absorption spectrophotometer (Perkin Elmer Lambda 25) in the 400–850 nm wavelength range. To find out resistance of gold nanorods to dimensional changes, purified sample was heated at 95 °C in a water bath for 2 h. Control GNRs were dispersed in phosphate buffer (pH 7.5). Presence of the rod morphology by UV–Vis spectroscopy was confirmed.

Zeta potential measurements of the particles were carried out on a Malvern Zeta Sizer (Nano ZS) at room temperature.

Immobilization of papain on gold nanorods

5 mg mL^{-1} papain solution in mixed buffer containing 50 mM each acetate, phosphate and glycine, pH 9.0, was incubated with 30 nm purified GNRs at room temperature for 2 h.

Enzyme bound to gold nanorods surface was measured determining the enzyme concentration in the supernatant after immobilization. The loss in absorbance at 280 nm in the supernatant was used to quantify the amount of bound enzyme on gold nanorods.

All samples were kept refrigerated until assay.

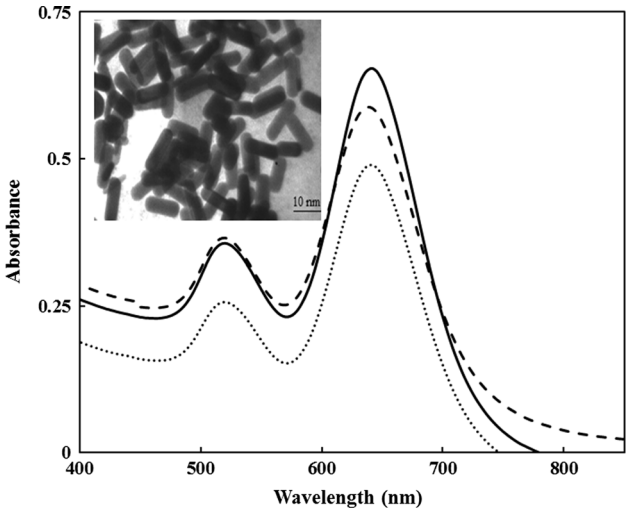

Fig. 1 Absorption spectra of gold nanorods (*solid line*); heated at 95 °C for 2 h (*dash dot line*); linked to papain (*dotted line*). In the inset: TEM image (TE 2000 Zeiss) of the purified GNRs

Protease activity measurements

Protease activity was determined according to the procedure of Arnon (Arnon 1970; Ramakrishna Nayak et al. 1979; Kembhavi et al. 1993; Nitsawang et al. 2006; Homaei et al. 2010). In a typical experiment, to 50 μL of enzyme solution diluted in 350 μL of 50 mM mixed buffer pH 9.0 containing 38 mM EDTA and 34 mM cysteine chloride, 400 μL of 1 % (w/v) aqueous solution of casein was added and the reaction mixture was incubated at room temperature for 10 min. The reaction was stopped by adding 800 μL of 10 % trichloroacetic acid solution. The mixture was incubated at room temperature for 30 min, centrifuged at 12,000 *g* for 10 min, to eliminate the insoluble non-hydrolyzed protein, while the measure of the soluble fraction, detected by UV measurement at 280 nm, represents a reliable method for papain activity, as widely reported by the above-reported bibliography.

One unit of protease was defined as the amount of enzyme that hydrolyzes casein to produce equivalent absorbance to 1 μmol of tyrosine/min using tyrosine as standard. In the case of the immobilized papain, the mixture was gently stirred during the reaction. Kinetic parameters were calculated applying the Michaelis–Menten equation and, in particular, the Lineweaver–Burk graph. k_{cat} value was determined by the ratio between the experimental V_{max} by papain concentration. An estimated molecular mass of 23,000 Da was adopted (Van Hekken et al. 1996).

Protein concentration was quantified by the Bradford method, using bovine serum albumin as standard (Bradford 1976).

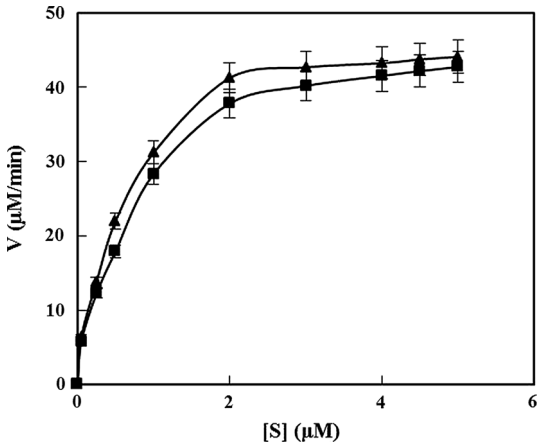

Fig. 2 Michaelis–Menten graph referred to free (*filled triangles*) and immobilized (*filled squares*) papain. Activity measurements were carried out at room temperature in mixed buffer, pH 9.0

Results

Papain immobilization

Inset of Fig. 1 shows TEM image of purified GNRs obtained as described in "Materials and methods".

Immobilization of papain from latex Carica papaya on GNRs was carried out simply mixing a relative concentrate solution of the enzyme with gold nanorods suspension for 2 h at room temperatures. Longer incubation time did not affect the surface coverage. Immobilization rate decreases in the presence of moderate concentration of NaCl (data not shown), indicating that ionic exchange effect plays an important role in papain immobilization.

Zeta potential value of the nanorods, measured at room temperature by electrophoretic light scattering technique, was +45.5 mV, a value that indicates a good stability of the colloidal dispersion.

Spectrophotometric characterization of heterogeneous catalyst

Figure 1 shows UV–Vis spectra of gold nanorods dispersion and compares their characteristic surface plasmon resonance bands after interaction with protein. Papain adsorption produces a slight change in the longitudinal surface plasmon resonance (LSPR) intensity of gold nanorods. In particular, after heating, gold nanorods tend to reshape in smaller nanostructure, but in our case the majority of them maintains their primary shape (dashed line): as a consequence the spectrum shows a slightly reduced intensity. Papain interacts with gold nanorods by electrostatic forces: positive surface of nanorods is neutralized by negative surface charges of papain (see "Discussion"), so changing the microenvironmental dielectric constant and the intensity of the absorption bands that depend on it, as Fig. 1 shows (dotted line).

The sensitivity of longitudinal plasmonic band to the changes in surrounding environment encourages the utilization of this method for the characterization of nanostructures in the development of novel nanobiosensors.

Catalytic activity measurements

Papain and its immobilized form revealed a Michaelis–Menten-type kinetic in the hydrolysis of casein (Fig. 2).

As shown in Table 1, where a summary of the stability differences between free and GNRs linked papain is reported; K_M and k_{cat} values, calculated by the Lineweaver–Burk plots, do not undergo significant variation after immobilization, on the contrary to that reported in literature for most enzymes (Stevanato et al. 1989; Reshmi et al. 2006; Agostinelli et al. 2007; Jiangwu et al. 2013; Illanes et al. 2013).

Figure 3, where the relative catalytic activity of free and immobilized papain at different pH values in the range of 2–12 is reported, shows in both the cases a bell-shape profile, characterized by maximum activity at pH 6.9 and 9.0 for free and immobilized papain, respectively. This last value was very similar to that found for papain immobilized on Sepharose (Homaei et al. 2010). Though free papain shows slightly higher catalytic activity than immobilized one, the catalytic performance of linked enzyme is well retained in a wider pH range between 2.0 and 12.0. In fact, at these extreme pH values, free papain shows relative residual activity <10 and 20 %, respectively, while in the case of immobilized enzyme values higher than 40 and 50 %, respectively, were found.

From Fig. 4, where the effect of temperature on the activity of free and linked papain is shown, it appears that maximum activity for immobilized enzyme was obtained at 70 °C, whereas it was ten degrees lower for free papain. The free form of the enzyme shows a relative higher activity at low temperature, but significantly decreases at temperatures higher than 60 °C; in the case of the immobilized enzyme, a relative lower activity at low temperatures and very higher activity at higher temperatures was found. In particular, at 30 and 90 °C, relative residual activity was about 70 and 30 %, respectively, for free papain, and about 40 and 80 % for the immobilized form.

From the Arrhenius plots (inset of Fig. 4), graphed utilizing the activity values in the temperature range 30–60 °C and 30–70 °C for free and immobilized papain, respectively, activation energy values of 1.87 and 2.53 kcal mol^{-1} K^{-1} for free and linked enzyme, respectively, were obtained.

As shown in Fig. 5a, b, where data of irreversible thermoinactivation at 80 and 90 °C are reported,

Table 1 Kinetic and stability parameters at different experimental conditions of free and gold nanorods immobilized papain from Carica papaya latex. k_{cat} and K_M values were determined by Lineweaver–Burk plots

Parameter	Free papain	GNRs immobilized papain
k_{cat} (min^{-1})	$2.8 \times 10^{-4} \pm 0.11$	$2.3 \times 10^{-4} \pm 0.17$
K_M (μM)	0.61 ± 0.03	0.66 ± 0.04
k_{cat}/K_M ($M^{-1}min^{-1}$)	$4.6 \times 10^2 \pm 0.12$	$3.5 \times 10^2 \pm 0.17$
pH maximum activity	6.9	9.0
Residual relative activity (%) at pH values 2 and 12	<10 and <20	≅40 and ≅50
Temperature maximum activity	≅60	≅70
Residual relative activity (%) at 30 and 90 °C	≅70 and 30	≅40 and 80
Activation energy values (kcal $mol^{-1}K^{-1}$)	1.87	2.53
Half-life (min) after 60 min storage at 90 °C	≅5	≅30
Half-life (min) after 60 min storage at pH values 3 and 12	<5 and <5	≅40 and 40
Residual activity (%) after 30 days storage at 4 and 22 °C	0 and 25	≅ 80
Residual activity (%) in the presence of 20 mM Ca^{2+}, Mg^{2+}, Ba^{2+}	10–20	38–57
Residual activity (%) in the presence of 20 mM Cu^{2+}, Zn^{2+}, Ni^{2+}, Mn^{2+}	0–10	16–20

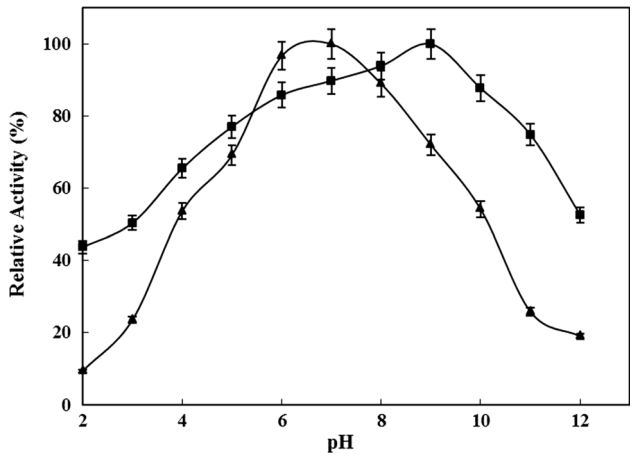

Fig. 3 Effect of pH on the activity of free (*filled triangles*) and immobilized (*filled squares*) papain. Activity measurements at different pH values were carried out in substrate saturation conditions at room temperature in mixed buffer

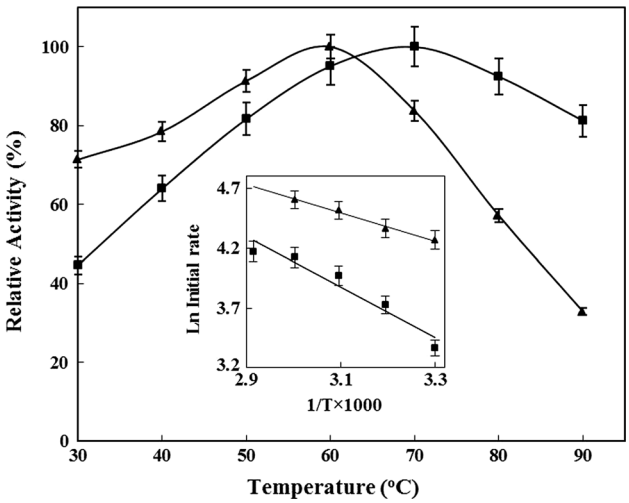

Fig. 4 Effect of temperature in the range 30–90 °C on the activity of free (*filled triangles*) and immobilized (*filled squares*) enzyme. Measurements were carried out in substrate saturation conditions in mixed buffer pH 9.0. In the inset, the respective Arrhenius plots (log V_{max} versus $1/T$) are reported

immobilized form of papain exhibited a marked increase in thermostability with time with respect to the free enzyme. At 90 °C, half-life of immobilized enzyme was about 30 min, while it was 5 min in the case of the free form. After 60 min incubation at 90 °C, immobilized enzyme retained 40 % of its initial activity, while negligible activity was observed in the case of the free enzyme.

Also in the case of incubation at extreme pH values 3.0 and 12.0 (Fig. 5c, d), it results that immobilized enzyme was more stable than the free form. In fact, after 60 min incubation, in both cases the immobilized papain retained about 40 % of residual activity, while; under the same conditions, <5 % for free papain was observed.

The storage stability of papain exhibited a significant increase after immobilization. As indicated in Fig. 6, free papain lost all of its initial activity after 50 and 30 days of incubation at 4 °C and room temperature, respectively; while, under the same conditions, immobilized papain preserves about 80 % of its original activity after 2 months of storage in both cases.

Relative activities of papain and its immobilized form in the presence of different concentrations of various bivalent metal ions, known as strong inhibitors of papain (Afaq and Iqbal 2001; Sluyterman 1967), are depicted in Table 2. In particular, 20 mM Ca^{2+}, Mg^{2+} Ba^{2+} reduces residual activity of about 80–90 % in the case of free enzyme and 43–62 % for the immobilized form. More enhanced is the difference when ions of the first transition series (Cu^{2+},

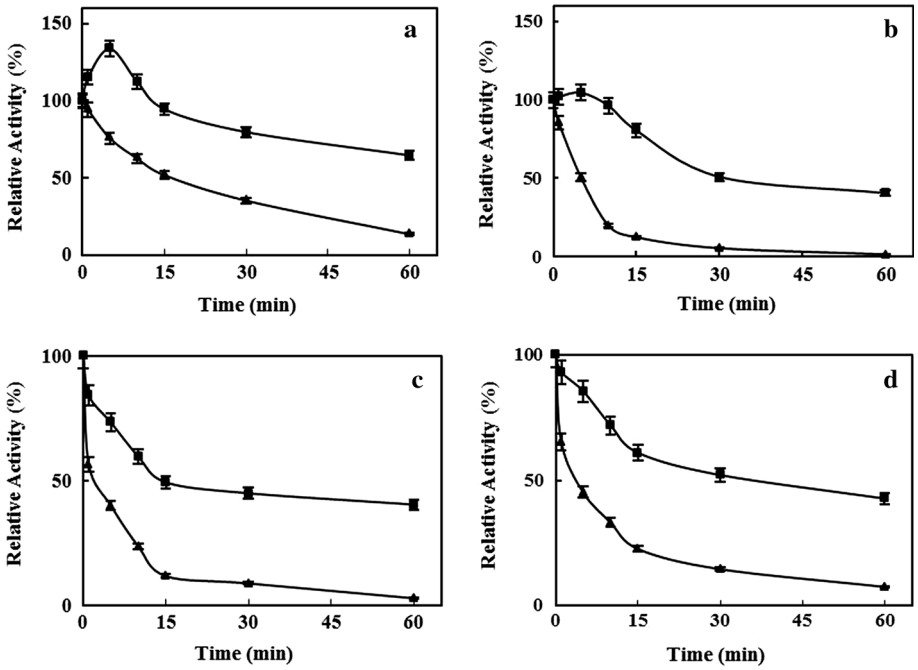

Fig. 5 Irreversible thermoinactivation at 80 °C (**a**) and 90 °C (**b**) and enzyme stability at pH 3.0 (**c**) and 12.0 (**d**) for free (*filled triangles*) and immobilized (*filled squares*) papain in mixed buffer. Native and linked papain were incubated at the different above-reported experimental conditions then aliquots of the enzyme were withdrawn at different times, cooled on ice, adjusted at pH 9.0 and the residual activity measured under the assay conditions in substrate saturation conditions. Control data were obtained measuring the activity of the same stock of enzyme solution kept for the same times on ice for thermal and at room temperature for the pH stability experiments

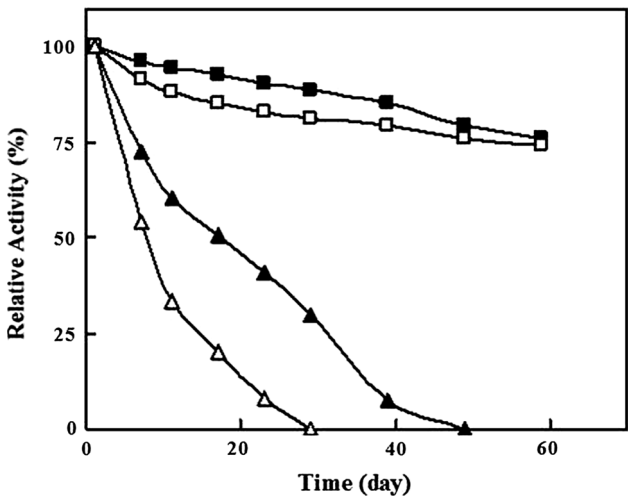

Fig. 6 Storage stability of free (*triangles*) and immobilized (*squares*) papain at 4 (*solid*) and 22 °C (*hollow*). Measurements were carried out in substrate saturation conditions

Zn^{2+}, Ni^{2+}, Mn^{2+}) at the same concentration were used; in this case, no residual activity for free enzyme incubated with Cu^{2+} and Ni^{2+} was found, while values of 5 and 10 % for Zn^{2+} and Mn^{2+}, respectively, were recorded. On the contrary, in the case of immobilized papain, residual activity values between 20 and 48 % were observed.

Discussion

The cationic surfactant plays an important role in the shape directing of nanostructures and forms bonds with surface of rods. Heating provides the energy required to change/break the bond between the micelles and the gold surface (Zou et al. 2010). Therefore, either the micelles around the longer rods will break or they will anneal around the shorter rods. This is simply statistical in nature, since longer GNRs have more points at which the decomposition can take place. Mohamed et al. (1998) reported that craft decomposition (dissolution) temperature of the most stable micelles is in the range of 155–160 °C and suggested that within this range the micelles encapsulating gold nanorods are completely destroyed. At this stage, the surface plasmon absorption band disappears and a black precipitate of aggregated gold powder is formed. Since our thermal stability experiments were carried out far below this temperature, it could be expected that only micelles surrounding the longer rods were melted/decomposed and rods of shorter length may still be present. Therefore, to maintain the rod morphology of nanostructures CTAB plays key role within a limited temperature range. Since the characteristic SPR bands of GNRs still exist after heating treatment, presence of the rod morphology has been assured for further kinetic and stability considerations of the protein at high temperature.

The so-prepared gold nanorods are then characterized by a bilayer of CTAB which provides their surface with positive charges and thus prevents nanorods aggregation in water by electrostatic repulsion. Then, the solvent-accessible faces of the nanorods are quaternary ammonium groups and a Zeta potential of +45.5 mV was found. Isoelectric point of papain is 8.75 indicating that, at our experimental conditions, i.e., pH 9.0, the protein is

Table 2 Effects of various metal chloride ions at different concentrations on the activity of free and GNRs linked papain. Measurements were carried out in substrate saturation conditions

Metal ion (mM)	Relative activity (%)	
	Free	Immobilize
Control (no add)	100	100
Ca^{2+}		
1	78	94
5	57	87
10	34	72
20	10	48
Mg^{2+}		
1	81	96
5	60	88
10	40	77
20	20	57
Ba^{2+}		
1	76	91
5	47	72
10	28	57
20	13	38
Cu^{2+}		
1	9	70
5	0	58
10	0	47
20	0	20
Zn^{2+}		
5	49	65
10	22	54
20	5	45
40	0	16
Ni^{2+}		
5	17	68
10	2	56
20	0	47
40	0	16
Mn^{2+}		
5	56	69
10	29	60
20	10	48
40	0	18

prevalently negatively charged. As a consequence, binding of papain to gold nanorods probably occurs via electrostatic interactions between the positively charged surface of the nanorods and the negatively charged enzyme, so as reported in literature referring to different support materials (Agostinelli et al. 2007; Gole and Murphy 2005; Alkilany et al. 2012).

Furthermore, cetyl residues, characterized by a 20 methylene length chains, create a highly hydrophobic environment which can favor interactions with hydrophobic zones of the enzyme, due to the presence of solvent-accessible non-polar amino acid residues in the primary structure.

Therefore, stabilization of papain on gold nanorods may occur through multipoint no-covalent electrostatic and hydrophobic interactions, that increase conformational rigidity and stabilize globular steric structure against particular environmental conditions (pH, temperature, etc.) able to denaturate proteins in native form (Sahoo et al. 2013; Salas et al. 2011; Bayramoglu et al. 2010; Homaei et al. 2010; Gabrovska et al. 2008; Rao et al. 2006; Sangeetha and Abraham 2006; Jiang et al. 2005; Leia et al. 2004). In fact, comparing to free form, the enzymatic activity of immobilized papain is higher for broader temperature and pH ranges, retaining about 50 % activity also for 60 days at 90 °C and more than 40 % activity at extreme pH values of 2 and 12.

The isoelectric point of the substrate casein is 4.6 at pH 9.0; it is strongly negatively charged and, as a consequence, for electrostatic reasons its concentration at the boundary layer of the positively charged support is higher than in the bulk solution. Furthermore, casein is relatively hydrophobic and the consequent interactions with the highly hydrophobic cetyl chain of CTAB can contribute to increase the substrate concentration around the support surface, that is, in correspondence of the immobilized enzyme (Talbert and Goddard 2012).

At low pH values, the higher activity of immobilized enzyme can be due to the microenvironmental rarefaction of H^+ ions because of ammonium ion-induced electrorepulsion and, as a consequence, the enzyme retains a higher activity also at apparent low pH values. At pH 2.0, the residual activity of linked enzyme is similar (45–50 %) to that recorded at pH 4.0 for free enzyme; i.e., positively charged surface of GNRs apparently reduces hydrogen ions concentration around linked papain of about two magnitude orders, i.e., two pH units.

At pH values >7, where a greater effect was observed, the microenvironmental substrate concentration results higher than in the bulk solution owing to the electroattractive effect between the positively charged surface and the negatively charged substrate; as a consequence, a higher activity than that recorded in homogeneous phase was found. In particular, the behavior of the activity with pH of linked papain appears shifted of two pH units toward alkaline values with respect to the free enzyme.

Kinetic parameters of linked papain appear extraordinary similar to those related to the free enzyme. The slight

increase in K_M value may be due to diffusion limitations, steric hindrance of the active site and/or loss of enzyme flexibility necessary for substrate binding (Cetinus and Oztop 2003; Jiang et al. 2005), while the decrease in k_{cat} could be due to the restriction for substrate to diffuse into the active site and the higher structural rigidity of immobilized enzyme compared to free enzyme. The catalytic efficiency (k_{cat}/K_M) of immobilized papain shows a lower decrease in activity compared to the free form.

On the other hand, linked to gold nanorods the enzyme shows higher catalytic efficiency (k_{cat}/K_M) as compared to that of other support (Cetinus and Oztop 2003; Reshmi et al. 2006; Wu et al. 2011; Jiangwu et al. 2013; Illanes et al. 2013). This could be due to the difference in size and surface chemistry of the nanostructures, since the modified rods have been synthesized with least required concentration of the surfactant in the presence of more silver ions. As far as the protein adsorption phenomenon is concerned, probable conformational changes and subsequent functional alterations would be directly dependent on the size and nature of the adsorbent. This is in accordance with earlier findings, showing that in the presence of zinc oxide nanoparticles of 4–7 nm size range, enzyme has only lost around 10 % of its activity (Roach et al. 2005). Furthermore, results of conformational changes nicely correlate with retention of more native-like enzyme activity in the case of adsorption on smaller nanorods (Gaoa et al. 2012).

Possibility of protein autolysis is reduced owing to lower freedom degrees consequent the immobilization on a solid support, i.e., enzyme molecules cannot collide because linked to the support and, as a consequence, the papain-autocatalyzed hydrolysis of the protein primary structure is almost impossible.

Inhibition data by divalent metal ions clearly indicate that the sensitivity of papain is reduced owing to immobilization process. Analogously to the stability to pH, lower sensitivity of immobilized enzyme toward divalent ions can be due to the GNRs surface characterized by diffuse positive charges that can drive back divalent ions creating a microenvironment around the enzyme characterized by a lower ion concentration.

By interpolation of the activity data in the presence of divalent metal ions (Table 2), it results that residual activity of immobilized enzyme in the presence of 20 mM Ca^{2+}, Mg^{2+}, Ba^{2+}, Zn^{2+}, Ca^{2+}, and Mn^{2+} corresponds to residual activity of free enzyme in the presence of the same ions at concentration values ranging between 5 and 10 mM; i.e., positive support apparently reduces ion concentration of a factor ranging between 2 and 4. This phenomenon appears more noticeable in the case of Cu^{2+} and Ni^{2+} for which the factor results more higher.

As a conclusion, the results here reported clearly demonstrate that immobilization of papain from Carica papaya latex on gold nanorods enhances enzyme stability and efficiency also at extreme experimental conditions (pH, temperature, presence of inhibitory divalent ions), opening new opportunities for biotechnological applications.

Furthermore, owing to the physicochemical characteristics of gold nanorods, the process of enzyme immobilization is simple, robust and applicable to other enzymes, thereby a promising material for enzyme immobilization.

Acknowledgments Authors are grateful to the University of Hormozgan for the financial support to this research.

Conflict of interest This work is free from any conflict of interest.

References

Afaq S, Iqbal J (2001) Immobilization and stabilization of papain on chelating sepharose: a metal chelate regenerable carrier. Electr J Biotech 4:120–124

Agostinelli E, Belli F, Tempera G, Mura A, Floris G, Toniolo L, Vavasori A, Fabris S, Momo F, Stevanato R (2007) Polyketone polymer: a new support for direct enzyme immobilization. J Biotechnol 127:670–678

Alkilany AM et al (2012) Gold nanorods: their potential for photothermal therapeutics and drug delivery, tempered by the complexity of their biological interactions. Adv Drug Deliv Rev 64:190–199

Arnon R (1970) Papain. Meth Enzymol 19:226–242

Bayramoglu G et al (2010) Reversible immobilization of glucose oxidase on polyaniline grafted polyacrylonitrile conductive composite membrane. Bioresour Technol 101:6881–6887

Billsten P et al (1999) Conformation of human carbonic anhydrase II variants adsorbed to silica nanoparticles. Langmuir 15:6395–6399

Blanco RM, Guisan JM (1992) Additional stabilisation of PGA-agarose derivatives by chemical modification with aldehydes. Enzyme Microb Technol 14:489–495

Bradford MM (1976) A rapid and sensitive method for the quantitation of microgram quantities of protein utilizing the principle of protein dye binding. Anal Biochem 72: 248–254

Cetinus SA, Oztop HN (2003) Immobilization of catalase into chemically crosslinked chitosan beads. Enzyme Microb Technol 32:889–894

Chakraborti S et al (2010) Structure and activity of lysozyme on binding to ZnO nanoparticles. Langmuir 26:3506–3513

Chen CC et al (2006) DNA-gold nanorod conjugates for remote control of localized gene expression by near infrared irradiation. J Am Chem Soc 128:3709–3715

Choma J et al (2012) Synthesis of rod-like silica—gold core-shell structures. Colloids Surf A 393:37–41

Delanoy G, Li Q, Yu J (2005) Activity and stability of laccase in conjugation with chitosan. Int J Biol Macromol 35:89–95

Dickerson EB et al (2008) Gold nanorod assisted near-infrared plasmonic photothermal therapy (PPTT) of squamous cell carcinoma in mice. Cancer Lett 269:57–66

Gabrovska K et al (2008) Encapsulation of glucose oxidase within poly (ethylene glycol) methyl ether methacrylate microparticles for developing an amperometric glucose biosensor. Int J Biol Macromol 43:339–345

Gaoa F et al (2012) Effect of surface oxide on the melting behavior of lead-free solder nanowires and nanorods. Appl Surf Sci 258: 7507–7514

Gole A, Murphy CJ (2004) Seed-mediated synthesis of gold nanorods: role of the size and nature of the seed. Chem Mater 16:3633–3640

Gole A, Murphy CJ (2005) Polyelectrolyte-coated gold nanorods: synthesis, characterization and immobilization. Chem Mater 17:1325–1330

Hauck TS et al (2008) Enhancing the toxicity of cancer chemotherapeutics with gold nanorod hyperthermia. Adv Mater 20:3832–3838

He W et al (2008) Two-photon luminescence imaging of bacillus spores using peptide-functionalized gold nanorods. Nano Res 1:450–456

Hinterwirth H et al (2012) Bioconjugation of trypsin onto gold nanoparticles: effect of surface chemistry on bioactivity. Anal Chim Acta 733:90–97

Hipwell MC, Harvey MJ, Dean PDG (1974) Affinity chromatography on a homologous series of immobilized N6-amega-aminoalkyl AMP. Effect of ligand–matrix spacer length on ligand–enzyme interaction. FEBS Lett 42:355–359

Homaei AA et al (2010) Cysteine enhances activity and stability of immobilized papain. Amino Acids 38:937–942

Huang X, Neretina S, El-Sayed MA (2009) Gold nanorods: from synthesis and properties to biological and biomedical applications. Adv Mater 21:4880–4910

Illanes CO et al (2013) Evidence of structural changes of an enzymatic extract entrapped into alginate beads. Biochem Eng J 70:23–28

Jiang DS et al (2005) Immobilization of *Pycnoporus sanguineus* laccase on magnetic chitosan microspheres. Biochem Eng J 25:15–23

Jiangwu Y et al (2013) The effect of various concentrations of papain on the properties and hydrolytic rates of β-casein layers l. Colloids Surf B 101:272–279

Kembhavi AA, Kulkarni A, Pant A (1993) Salt-tolerant and thermostable alkaline protease from *Bacillus subtilis* NCIM no.64. Appl Biochem Biotechnol 38:83–92

Kim J, Grate JW, Wan Pg (2006) Nanostructures for enzyme stabilization. Chem Eng Sci 61:1017–1026

Kotal M (2011) Fabrication of gold nanoparticle assembled polyurethane microsphere template in trypsin immobilization. J Nanosci Nanotechnol 11:10149–10157

Larsericsdotter H, Oscarsson S, Buijs J (2001) Thermodynamic analysis of proteins adsorbed on silica particles: electrostatic effects. J Colloid Interface Sci 237:98–103

Leia H et al (2004) The preparation and catalytically active characterization of papain immobilized on magnetic composite microspheres. Enzyme Microb Technol 35:15–21

Li Z et al (2009) RGD-conjugated dendrimer-modified gold nanorods for in vivo tumor targeting and photo-thermal therapy. Mol Pharm 7:94–104

Lv M et al (2009) Trypsin-gold nanoparticle conjugates: binding, enzymatic activity, and stability. Prep Biochem Biotechnol 39:429–438

Mahmoud KA et al (2013) Preparation of well-dispersed gold/magnetite nanoparticles embedded on cellulose nanocrystals for efficient immobilization of papain enzyme. Appl Mater Interfaces 5:4978–4985

McKenzie F (2009) Quantitation of biomolecules conjugated to nanoparticles by enzyme hydrolysis. Chem Commun (Camb) 28:2872–2874

Mohamed MB et al (1998) Thermal reshaping of gold nanorods in micelles. J Phys Chem B 102:9370–9374

Nikoobakht B, El-sayed MA (2003) Preparation and growth mechanism of gold nanorods (NRs) using seed-mediated growth method. Chem Mater 15:1957–1962

Nitsawang S, Hatti-Kaul R, Kanasawud P (2006) Purification of papain from Carica papaya latex: aqueous two-phase extraction versus two-step salt precipitation. Enzyme Microb Technol 39:1103–1107

Pissuwan D, Valenzuela SM, Cortie MB (2008) Prospects for gold nanorod particles in diagnostic and therapeutic applications. Genet Eng Rev 25:93–112

Pissuwan D, Niidome T, Cortie MB (2011) The forthcoming applications of gold nanoparticles in drug and gene delivery systems. J Control Release 149:65–71

Ramakrishna Nayak B, Mallikarjuna Rao N, Pattabiraman (1979) Studies on plant gums. proteases in neem (*Azadirachta indica*) gum. J Biosci 1:393–400

Rao RS et al (2006) Enzymatic activities of proteases immobilized on tri (4-formyl phenoxy) cyanurate. Enzyme Microb Technol 39:958–962

Reshmi R, Sanjay G, Sugunan S (2006) Enhanced activity and stability of a-amylase immobilized on alumina. Catal Commun 7:460–465

Roach P, Farrar D, Perry CC (2005) Surface tailoring for controlled protein adsorption: effect of topography at the nanometer scale and chemistry. J Am Chem Soc 127:8168–8173

Rocha JMS, Gil MH, Garcia FAP (1998) Effects of additives on the activity of a covalently immobilized lipase in organic media. J Biotechnol 66:61–67

Sahoo B et al (2013) A novel approach for efficient immobilization and stabilization of papain on magnetic gold nanocomposites. Colloids Surf B 101:280–289

Salas PT et al (2011) Immobilized biocatalysts: novel approaches and tools for binding enzymes to supports. Adv Mater 23:5275–5282

Sangeetha K, Abraham TE (2006) Chemical modification of papain for use in alkaline medium. J Mol Catal B Enzym 38:171–177

Sau et al (2004) Newly synthesized water soluble cholinium-purpurin photosensitizers and their stabilized gold nanoparticles as promising anticancer agents. Langmuir 20:6414–6420

Sluyterman LA (1967) The activation reaction of papain. Biochim Biophys Acta 139:430–438

Stevanato et al (1989) Characterization of free and immobilized amine oxidases. Biotech Appl Biochem 11:266–272

Takahashi H, Niidome Y, Yamada S (2005) Controlled release of plasmid DNA from gold nanorods induced by pulsed near-infrared light. Chem. Commun 7(17):2247–2249

Talbert JN, Goddard JM (2012) Enzymes on material surfaces. Colloids Surf B 93:8–19

Van Hekken DL, Strange ED, Lu DP (1996) Functional properties of chemically phosphorylated whole casein. J Dairy Sci 79:1049–1942

Wilchek M, Miron T (2003) Oriented versus random protein immobilization. J Biochem Biophys Methods 55:67–70

Wu C et al (2011) Size-modulated catalytic activity of enzyme nanoparticle conjugates: a combined kinetic and theoretical study. Chem Commun 47:7446–7448

Yu C, Irudayaraj J (2007) Multiplex biosensor using gold nanorods. Anal Chem 79:572–579

Zou R et al (2010) Thermal stability of gold nanorods in an aqueous solution. Colloid Surf A 372:177–181